Journal of Hazardous Materials 403 (2021) 123941

Contents lists available at ScienceDirect

Journal of Hazardous Materials

journal homepage: www.elsevier.com/locate/jhazmat

A split aptamer (SPA)-based sandwich-type biosensor for facile and rapid detection of streptomycin

Qian Zhu [a], Lanhua Liu [a], Ruoyu Wang [a], Xiaohong Zhou [a,b,*]

[a] State Key Joint Laboratory of ESPC, School of Environment, Tsinghua University, Beijing, 100084, China
[b] National Engineering Laboratory for Advanced Technology and Equipment of Water Environment Pollution Monitoring, Changsha, 410205, China

ARTICLE INFO

Editor: R. Teresa

Keywords:
Sandwich-type biosensor
Evanescent wave
Split aptamer
Streptomycin

ABSTRACT

As antibiotic pollution is gaining prominence as a global issue, the demand for detection of streptomycin (STR), which is a widely used antibiotic with potential human health and ecological risks, has attracted increasing attention. Aptamer-based biosensors have been developed for the detection of STR in buffers and samples, however, the non-target signals due to the conformational variation of free aptamers possibly affect their sensitivity and stability. In this study, by introducing the STR-specific split aptamer (SPA), a sensitive evanescent wave fluorescent (EWF) biosensor is developed for the sandwich-type based detection of STR. The standard calibration curve obtained for STR has a detection limit of 33 nM with a linear range of 60–526 nM. This biosensor exhibited good selectivity, reliable reusability for at least 100 times measurements, and high recovery rates for spiked water samples; moreover, all detection steps are easy-to-operate and can be completed in 5 min. Therefore, it exhibits great promise for actual on-site environmental monitoring. Additionally, without introducing any other oligonucleotides or auxiliary materials, this SPA-based biosensing method shows potential as a simple, sensitive, and low-cost manner for the detection of other small molecular targets.

1. Introduction

Streptomycin (STR) is an aminoglycoside antibiotic used to treat gram-negative bacteria infections. Currently, STR is widely used in medicine, animal husbandry, and agriculture (van Bruijnsvoort et al., 2004; Ferguson et al., 2002). However, STR residues in food and the aquatic environment may cause side effects in humans and animals, including toxicity that impairs hearing and damages nerves and kidneys (Yamamoto-Fujita and Kumar, 2005). Moreover, because of its high water solubility, STR residues in the aquatic environment are difficult to completely remove. Thus, the efficient and accurate detection of STR in water samples is essential for environmental monitoring and to protect human health. Traditional techniques to detect STR, such as high-performance liquid chromatography (HPLC), gas chromatographic-mass spectrometric (GC—MS), and spectrophotometry methods have been developed and widely used (Preu and Petz, 1999; Abbasi and Hellenäs, 1998; Li and Gao, 2008); nevertheless, those techniques rely on large and expensive precision instruments and professional operators, which are not suitable for on-site analyses or automated water-quality monitoring (Capodaglio et al., 2016; Yagur-Kroll et al., 2015). Compared with instrumental technologies, aptamer-based biosensors (aptasensors) have attracted considerable attention because of their rapid, simple, accurate, and low-cost advantages (Mehlhorn et al., 2018; Paniel et al., 2013; Feng et al., 2014a; Ping et al., 2015; Meirinho et al., 2016). Aptamers are mainly single-strand DNA or RNA probes selected by *in vitro* methods, which can specifically combine with target molecules. Based on the high selectivity and sensitivity of aptamers, aptasensors have been developed for the detection of various targets, including heavy metals, small molecules, and proteins, showing potential prospects in the field of environmental monitoring, medical diagnosis, food safety and so on (Mehlhorn et al., 2018; Hong et al., 2012; Nguyen et al., 2017; Abdul Ghaffar Memon et al., 2019; Bayramoglu et al., 2015, 2019a; Ozalp et al., 2015; Bayramoglu et al., 2019b). Because the first aptamer for STR was reported by Wallace and Schroeder in 1998, several aptasensors have been developed for trace STR detection in milk, honey, and water samples, among others (Ferguson et al., 2002; Wallace and Schroeder, 1998; Danesh et al., 2016; Emrani et al., 2016; Strehlitz et al., 2012). Zhou and co-workers reported a STR-specific aptasensor by using a gold nanoparticle-based colorimetric method, and detected STR in honey at a range of 0.2–1.2 μM (Zhou et al., 2013). Lin et al. developed a fluorescent aptasensor for STR detection by using an ssDNA aptamer and its complementary sequence,

* Corresponding author at: State Key Joint Laboratory of ESPC, School of Environment, Tsinghua University, Beijing, 100084, China.
E-mail address: xhzhou@mail.tsinghua.edu.cn (X. Zhou).

https://doi.org/10.1016/j.jhazmat.2020.123941
Received 22 June 2020; Received in revised form 31 August 2020; Accepted 1 September 2020
Available online 13 September 2020

with the limit of detection (LoD) of 94 nM (Lin et al., 2018). However, the dynamic conformational changes of free aptamers may lead to non-target signals, especially in the case of small-molecule targets, which present challenges for both the LoDs and practical applications of STR aptasensors (Chen et al., 2016; Wang et al., 2019).

A split aptamer (SPA), generated by splitting the parent aptamer, is a pair of oligonucleotide fragments that recognize the same target and are assembled together. Compared with the parent aptamers, the short SPAs are easier to synthesize and exhibit more stable conformations (Wang et al., 2018); moreover, SPAs are suitable for the sandwich-type recognition mechanism with high specificity (Chen et al., 2016). In recent years, some SPAs have demonstrated excellent capability with different transduction methods, including colorimetry, fluorescence, and electrochemical methods (Chen et al., 2016; Chen and Zeng, 2013; Cheng et al., 2013; Wu et al., 2013; Feng et al., 2014b; Yang et al., 2015). The sandwich-type design, optimized structure, and low cost of SPAs are valuable for the design of more sensitive, stable, and simple STR aptasensors. Piganeau and Tereshko first reported the STR-specific SPA (Tereshko et al., 2003; Piganeau and Schroeder, 2003), the stability of which was further investigated by Nick via molecular dynamics simulation and single-molecule force spectroscopy (Nick et al., 2016). It provided the basis for designing the optimized dual recognition sensing mode.

Optical biosensors have received considerable attention during the past few decades because of their potential application in environmental monitoring, food safety, and medical diagnostics. Among them, evanescent wave fluorescent biosensors have been extensively studied because of their high sensitivity, good selectivity, and easy-to-miniaturize capability (Liu et al., 2014; Wang et al., 2015a; Liu et al., 2017a, 2018). In this type of biosensor, the evanescent wave serves as excitation energy, whereas fluorophore acts as a donor, and the emitted fluorescent signals can be quantitively determined and correlated with target concentrations. Because the evanescent wave is a near-surface phenomenon, only fluorophore-labeled targets captured on the surface exhibited fluorescent signals, indicating that this type of biosensor could offer remarkable sensitivity and selectivity. We have developed an evanescent wave fluorescent (EWF) biosensor. The proposed EWF biosensor system provided a more integrated configuration than those previously reported (Kronick and Little, 1975; Taitt et al., 2005; Song et al., 2007; Long et al., 2008). By integrating recognition elements, such as antibodies and functional nucleic acids, this EWF system sensitively detected many contaminants of widespread concern, including sulfadimidine, mycotoxin, microcystin-LR, and heavy metal ions, among others (Liu et al., 2014, 2015; Wang et al., 2015b, a; Liu et al., 2017b). However, the single recognition mode based on the one small-molecule binding site of most biological materials may lead to tedious detection procedures and inferior sensitivity.

Based on our previous work, our objective was to establish an SPA-based sandwich-type biosensor for the facile and rapid detection of STR. By combining an effective STR-specific SPA with evanescent wave fluorescence sensing methods, this SPA-based sandwich-type biosensor could detect STR in buffers and real-water samples with high sensitivity and good selectivity. It is noted that without pre-reaction, this biosensor has the advantages of simple operation and fast detection speed (within 5 min per sample), exhibiting broad prospects for actual on-site antibiotic monitoring. Moreover, this SPA-based detection method does not need to introduce any extra helper oligonucleotides, which can be extended to develop aptasensors for other small-molecule contaminants by using different SPA materials.

2. Material and methods

2.1. Reagents

Bovine serum albumin (BSA), glutaraldehyde (25 % aqueous solution), 3-aminopropyl-triethoxysilane (APTS), penicillin G (PNG), kanamycin A (KNA), tetracycline (TC), tobramycin (TOB), neomycin (NEO), streptomycin (STR), tris-(hydroxymethyl) aminomethane (Tris), and metal salts (NaCl, KCl, $MgCl_2$) were purchased from Sigma Aldrich (USA). Sodium cyanoborohydride and glycine were obtained from AMRESCO (USA). Cy5.5 NHS ester was purchased from GE Healthcare Life Sciences (USA). BupH™ Phosphate Buffer Saline (PBS) packs were obtained from Thermo Fisher Scientific (USA). Other chemicals used for buffers and solvents were obtained from J&K (China). All solutions were prepared using molecular-grade ultrapure sterilized water (Corning Cellgro, USA).

The isoelectric BSA blocking solution was prepared by dissolving BSA in 0.1 M sodium citrate/citric acid buffer (pH 4.6) and the final concentration was 2 mg mL^{-1}. Three types of buffers were used based on our previous studies (Wang et al., 2019, 2015c). The 0.1 M PBS stock solution was prepared by dissolving one BupH™ PBS pack in 500 mL molecular-grade water, and 10 mM PBS buffer (pH 7.4) diluted by PBS stock solution was used in experiments. The 10 mM PBS buffer (pH 7.4) was selected as a model buffer to ensure a stable baseline, and a sodium dodecyl sulfate (SDS) buffer (pH 1.9) was used as a wash buffer to regenerate the sensing surface (Wang et al., 2015c). The 10 mM Tris-HCl buffer (pH 7.2) functioned as a binding buffer to ensure the binding between streptomycin and nucleic acid probes (Wang et al., 2019).

Oligonucleotides of STR-specific split aptamers (HPLC grade) were synthesized by Dalian Takara Biomedical Technology (China), and these sequences and others used in this study are listed in Table 1.

2.2. Instrument

The EWF biosensing platform has been described in our previous studies (Wang et al., 2015c, b; Wang et al., 2017). Briefly, as shown in Fig. 1A, an 8 mW pulse diode laser was switched on to generate a laser beam at 635 nm. The laser light was directly launched into a single-mode fiber and then coupled into the multimode fiber. Considering that the laser beam propagated via total internal reflection (TIR), an evanescent field was generated and provided the energy for fluorophore emission on the fiber surface. The emitted fluorescent signals were captured by the same optical fiber and quantified via the lock-in amplifier. This surface-modified optical fiber was embedded inside a glass flow cell, where samples and buffers were shifted and delivered by a pump and a multi-ported valve. A built-in computer was used to control the entire process.

The quartz optical fiber (8.5 cm in length, 600 μm in diameter) used in the EWF biosensor was purchased from Chunhui Science & Technology Industrial (China).

2.3. Modification of the optical fiber

To form a sensing area, the size and structure of fiber were first modified. The fiber, with the coating removed from 3.5 cm along one end, was etched in hydrofluoric acid (HF) for approximately 2.5 h to form a tapered structure and produced a sensing region with a diameter of 220 μm to meet the tapered ratio with maximum fluorescence collection capacity (Long et al., 2008). The size of etched fibers was measured by the microscope every 20 min during the process of tube-etching until the final diameter of 220 μm. Then, the etched fibers were thoroughly washed with ultrapure water and dried in an oven.

Before the RNA probe modification of fibers, it was essential to clean the tapered fibers with piranha solution (3:1 mixture of H_2SO_4 and 30 %

Table 1
Oligonucleotides used in this study for STR sensing.

Name	Sequence (5′-3′)
$SPA1_{STR}$	NH_2-$(CH_2)_6$-CGGCACCACGGUCGGAUC
$SPA2_{STR}$	Cy5.5-GAUCGCAUUUGGACUUCUGCC
A20	Cy5.5-AAAAAAAAAAAAAAAAAAAA

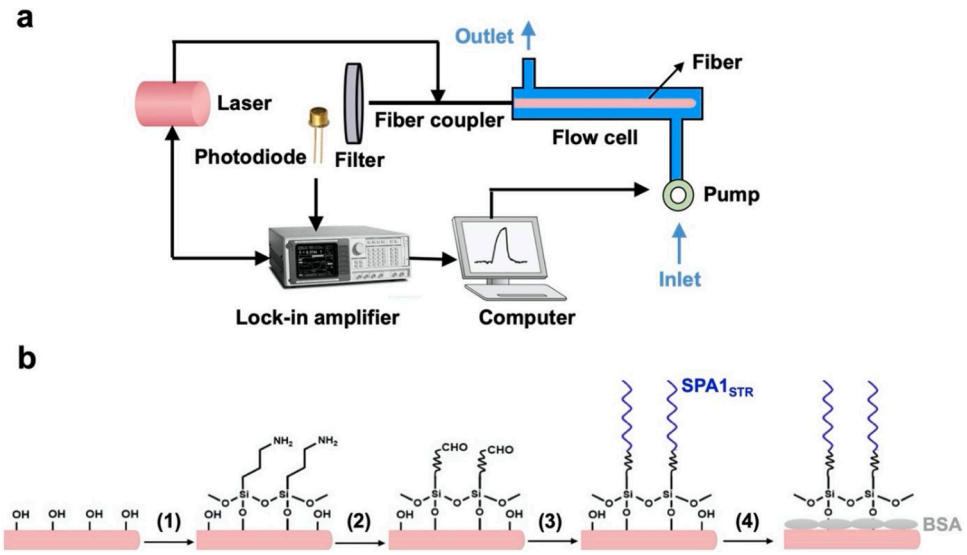

Fig. 1. (a) Schematic of the EWF platform. (**b**) The process of $SPA1_{STR}$ modification of fibers. The process numbers in **1b** correspond to the modification process above.

H_2O_2) to remove any surface residues. The four steps for the modification are described below.

(1) The tapered fiber region was immersed in a 1 % v/v solution of APTS (in dry toluene, 2 h, 25 °C) for aminosilanization. Next, the fibers were thoroughly washed and then sonicated in toluene for 15 min. Then, the APTS-modified fibers were dried with nitrogen and fixed by heating (1 h, 200 °C).
(2) To introduce the aldehyde groups, the fibers were immersed in 1 % v/v glutaraldehyde aqueous solution (Long et al., 2008) overnight in a shaker (37 °C, 90 rpm) and then thoroughly washed with ultrapure water.
(3) The aldehyde-activated fibers were immersed in $SPA1_{STR}$ solution overnight in a shaker (37 °C, 90 rpm) to immobilize $SPA1_{STR}$ molecules by the formation of a Schiff base and then thoroughly washed with ultrapure water.
(4) Before use, the optical fibers were blocked by isoelectric BSA solution in a shaker (37 °C, 4 h, 90 rpm).

2.4. Characterization of the surface modification of optical fibers

The element compositions and chemical states of optical fiber at different steps of surface modification were determined by X-ray photoelectron spectroscopy (XPS, Thermo Escalab 250Xi, USA). Before analysis, the XPS spectra were calibrated by a C 1s peak at 284.8 eV. Atomic force microscopy (AFM, Bruker Dimension FastScan, German) was further used to observe the surface morphology of optical fibers before and after modification.

2.5. Performance evaluation

2.5.1. Sensitivity

STR at various concentrations and 2 μL $SPA2_{STR}$ stock solution of 100 μM were added into 450 μL aliquots of Tris-HCl buffer (10 mM Tris, 250 mM NaCl, 5 mM $MgCl_2$, pH 7.2). After simple incubation, fluorescence intensity was measured by the EWF platform. The testing process was described as follows. Firstly, the 10 mM PBS buffer (pH 7.4) was pumped at a constant flow rate of 20 μL s^{-1} for more than 10 s to ensure a stable baseline, then samples were pumped into the EWF biosensing platform in 15 s at a constant flow rate of 20 μL s^{-1} and then the pump was set to stop for 2 min for surface-based STR recognition as well as fluorescence excitation, during which the fluorescence intensity of each sample was monitored, and the fluorescence signal at the end of 2 min reaction were recorded as the indicator for quantitate detection. After each measurement, a regeneration process was performed by a 60 s washing with the SDS buffer (0.5 %, pH 1.9) and a 40 s pumping of 10 mM PBS buffer (pH 7.4) to stabilize the baseline again.

2.5.2. Selectivity

To investigate the selectivity, five different types of antibiotics, including PNG, TC, TOB, NEO, and KNA, were added to the sensing solution individually at concentrations of 100 nM and the differences in fluorescence intensity were analyzed. Fluorescence intensities for other antibiotics were normalized by that of 100 nM STR as an index to indicate the selectivity. Detection procedures were performed based on the same conditions as described in methods of sensitivity assay.

2.5.3. Environmental samples

Five sources of real-water samples, including mineral spring water (NongfuSpring, China), bottled purified water (Wahaha, China), tap water (our lab, Tsinghua University, China), surface water (Hetang Lake, Tsinghua University, China), and wastewater (Sewage well, Tsinghua University, China), were selected to investigate the practicability of the developed biosensor. Before analysis, water samples were filtered using a 0.22 μm filter and then mixed with 10X Tris-HCl buffer in a ratio of 9:1. Next, 2 μL $SPA2_{STR}$ stock solution of 100 μM was added to 450 μL of samples, and measurements were taken by the established EWF aptasensor. Detection procedures were performed based on the same conditions as described in methods of sensitivity assay. To improve the accuracy, all measurements were performed in triplicate, and results were expressed as an average with the standard deviation.

3. Results and discussion

3.1. Characterization of $SPA1_{STR}$-modified optical fiber

The surface element compositions and chemical states of optical fiber at different steps of modification were investigated by XPS spectra. As shown in Fig. 2a, the P2p and N 1s peaks existed after RNA modification and BSA blocking. For the P2p spectrum (Fig. 2b), a weak peak at 134.2 eV was detected after RNA modification (the black line), which certified the existence of nucleic acid on the surface of the fibers after modification. Fig. 2c represents the N 1s peak at 400.1 eV in a high-resolution spectrum, which was increased by a large amount after

blocking with N element-rich BSA protein. Additionally, the O 1s and Si 2p high-resolution spectra are also presented in Fig. 2d and e. Combined with the difference in element content shown in Fig. 2f, the surface modification of fibers was considered successful.

Furthermore, AFM testing was selected to observe the surface morphology of fibers before modification, during the different steps of modification, and after regeneration; the results are shown in Fig. 3. The bare fiber showed a relatively flat surface with a height range (*dh*) around 5.0 nm. After aldehyde activation, no significant difference was found (*dh* $ 4.4 nm) because of the small size of the introduced chemicals. The height range became larger after RNA modification (*dh* $9.0 nm), and BSA blocking greatly increased the height range to 38.7 nm because of the binding of BSA protein on the surface of fibers. It retained a relatively stable surface morphology before and after use as shown in Fig. 3d and e. Besides the *dh*, roughness average (Ra), RMS roughness (Rq) were also selected to evaluate the surface roughness, and obtained similar conclusion as above.

3.2. Sensing mechanism

Based on the specific binding affinity of this SPA and STR reported in the previous studies (Tereshko et al., 2003; Nick et al., 2016), the sandwich-type detection of STR in a facile and rapid sensing manner was proposed on the EWF biosensing platform. The schematic diagram of the methodology is shown in Fig. 4a. $SPA1_{STR}$ (in blue), a fragment of the STR-specific split aptamer, was immobilized on the optical sensing interface by covalent binding methods, and a C6 linker with 6 carbons were introduced to the 5′ termini of $SPA1_{STR}$ to completely expose the SPA structure with sufficient flexibility (Wang et al., 2017).

Another SPA fragment, $SPA2_{STR}$ (in pink), was labeled with Cy5.5

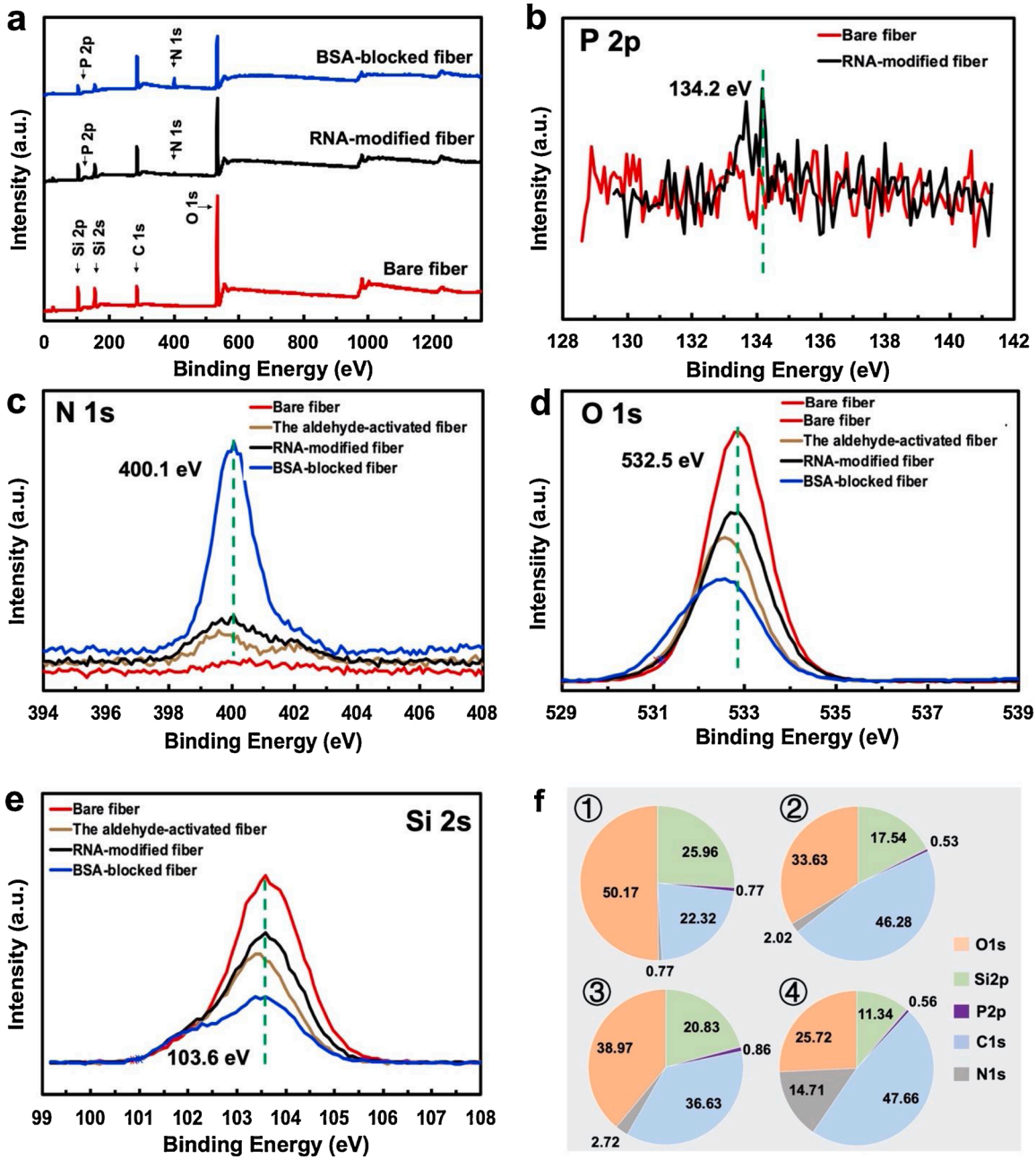

Fig. 2. XPS spectra of fibers at different steps including ① bare fiber, ② the aldehyde-activated fiber, ③ RNA-modified fiber, and ④ BSA-blocked fiber, were presented. a) survey; b) P 2p; c) N 1s; d) O 1s; e) Si 2s; f) Atomic components (%).

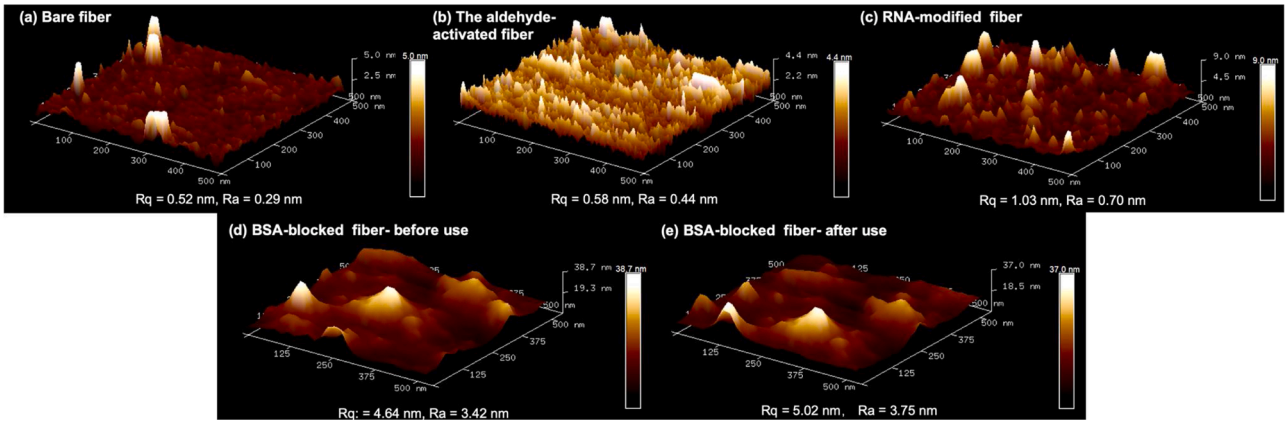

Fig. 3. AFM images of different five different fibers, including (a) bare fiber, (b) the aldehyde-activated fiber, (c) RNA-modified fiber, (d) BSA-blocked fiber before use and (e) after 100 times regeneration, were presented. The obtained AFM data were analyzed using NanoScope Analysis 1.8, and Height ranges (*dh*) of each area was calculated. Two other profile roughness parameters, including roughness average (*Ra*), RMS roughness (*Rq*) were labeled in the bottom of each figure.

and mixed with samples in a solution for the sandwich-type recognition of STR. Because the intensity of the evanescent field decreased exponentially with distance away from the interface (Kronick and Little, 1975), only Cy5.5 molecules bound to the sensing surface were excited. In the presence of STR, the Cy5.5-labeled $SPA2_{STR}$ assembly formed a sandwich-type ternary with the surface-immobilized $SPA1_{STR}$ and STR on the fiber surface, emitting detectable fluorescence signals recorded by a built-in computer. The fluorescent intensity reflected the concentration of STR. Conversely, in the absence of STR, it was difficult to form stable composite structures between the two SPA fragments on the sensing surface, which led to a very low signal collected by the biosensor. After the detection of one sample, the attached $SPA2_{STR}$ and STR were dissociated in a continuous flow of 0.5 % SDS buffer (pH = 1.9). In this turn-on detection method, concentrations of STR were positively correlated with fluorescence intensity in a broad detection range. This SPA-based sandwich-type detection method did not need any pre-reaction, exhibiting obvious advantages of simple operation and fast detection.

The proof-of-concept experiments were conducted to confirm the sensing mechanism. As shown in Fig. 4b, when an STR sample with the non-complementary sequence A20 was pumping through the flow cell, the fluorescence intensity stabilized at a very low level (in red); conversely, when adding $SPA2_{STR}$ solutions with STR, the fluorescence was greatly enhanced because of the sandwich-type recognition of $SPA1_{STR}$, $SPA2_{STR}$, and STR (in black). It was indicated that the sandwich-type recognition based on the SPA_{STR} was highly reliable and specific. Moreover, the low fluorescence of A20 illustrated the low non-specific adsorption of the fiber sensing interface, proving that the modified fiber was successfully blocked by isoelectric BSA. It should be noted that since the introduction of the isoelectric BSA blocking method to the DNA-based optical-fiber modification was reported with successfully enhanced sensing performance (Wang et al., 2017), the blocking method was further applied to block the sandwich-type and RNA-modified fiber and effectively avoided the noises caused by non-specific adsorption.

The entire detection cycle is presented below (**Figure S1**). The laser was switched on at the beginning of STR measurements. Before the detection of each sample, 10 mM PBS buffer was pumped through the flow cell until a stable fluorescence background was achieved. Then, a 450 μL sample mixed with $SPA2_{STR}$ was delivered to the cell at 1.5 mL min^{-1} until the cell was filled with the test sample. Next, the pump was turned off for the sandwich recognition of STR on the surface of an $SPA1_{STR}$-modified optical fiber and fluorescence signals were recorded. After every measurement, SDS buffer (pH 1.9) was pumped to elute the captured $SPA2_{STR}$ and STR from the fiber surface for 1 min to ensure the regeneration of the sensing interface. The total time for this detection procedure was less than 5 min (Fig. 4b).

3.3. Sensitivity

According to the established streptomycin detection scheme, the sensitivity of this established method was investigated. Without pre-

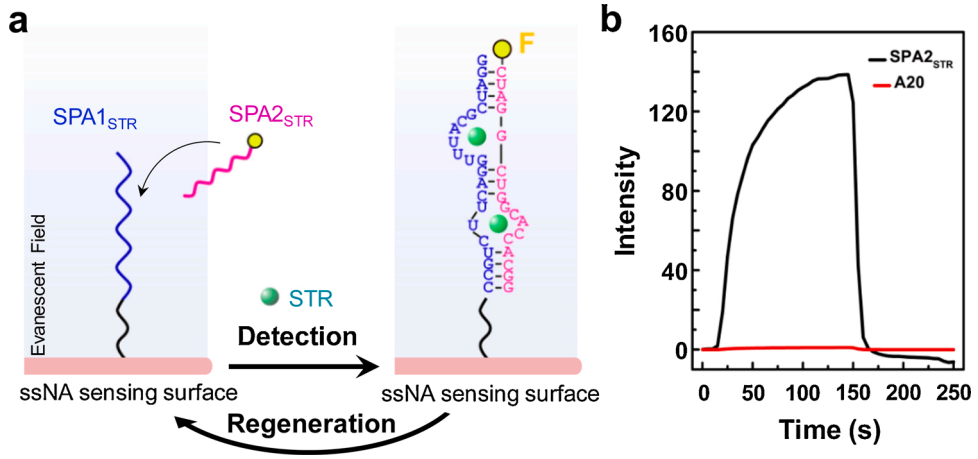

Fig. 4. (a) Schematic of SPA-based sandwich-type biosensor for detection of STR. (b) Real-time fluorescent signals with A20 sequence (in red) and $SPA2_{STR}$ (in black), both samples contained 100 nM STR in 450 μL 10 mM Tris-HCl buffer (pH 7.2).

reaction, samples containing STR were directly mixed with $SPA2_{STR}$ reagent and then delivered into the EWF biosensor for measurement. As expected, the fluorescence intensity was positively correlated with the concentration of STR. A four-parameter logistic fitting was used to quantify STR, and the collaboration curve of fluorescence intensity vs STR concentrations is shown in Fig. 5a. In the logistic-fitted collaboration, the signal at 10 % of the maximal signal (EC10) was defined as the limit of detection (LoD), and signals from 20 % to 80 % were used to define the linear working range. By calculation, the LoD of this SPA-based biosensor was 33 nM, and the linear relationship was observed in the range of 60–526 nM.

As illustrated in Table 2, relative to other STR sensors, this biosensor showed comparable sensitivity. Additionally, this SPA-based detection mode has advantages of no pre-reaction, simple operation, and fast detection speed, indicating that this established biosensor could be sensitive enough to monitor the STR contaminants quickly in water and food.

3.4. Selectivity

To evaluate the selectivity of the sensing system for STR detection, other environmentally relevant antibiotics, including PNG, TC, TOB, NEO, and KNA, were detected instead of the target under the same conditions.

SPAs were shown to be highly specific for target binding and have been reported as recognition elements in the detection of ATP, cocaine, and adenosine, among others (Chen et al., 2016; Bai et al., 2014; Zhang et al., 2008; Zuo et al., 2009). By the combination of STR-specific SPA and EWF biosensing platform, this SPA-based biosensor was expected to be highly specific for STR sensing. As expected, in the selectivity trials, 100 nM STR significantly changed the fluorescence intensity (see Fig. 5b). In contrast, other selected antibiotics at the same concentration (including PNG, TC, TOB, NEO, and KNA) generated less than 10 % fluorescent intensity compared to that of STR. These results suggest that this biosensor displayed highly favorable and specific recognition of STR among common antibiotics.

Table 2
Several methods of streptomycin nucleic acid-sensing based on nucleic acid aptamers.

Sensing mode	Principle	LoDs (nM)	Ref
Colorimetric	Unmodified gold nanoparticles	200	Zhou et al. (2013)
Electrochemistry	Porous carbon nanorods graphene-based signal enhancement	0.05	Yin et al. (2016)
Electrochemistry	Arch nuclease digestion system	11.8	Mohammad Danesh et al. (2016)
Photoelectricity	CdTe quantum dot and Single-wall carbon nonglue	0.033	Xu et al. (2017)
Fluorescence	Gold nanoparticles quench surface fluorophore	47.6	Asnaashari et al. (2018)
Fluorescence	Double-stranded nucleic acid fluorochrome	54.5	Taghdisi et al. (2016)
Fluorescence	SPA-based evanescent wave fluorescent biosensor	33	This study

3.5. Regeneration

Because of the reversible association of STR and split aptamers ($SPA1_{STR}$, $SPA2_{STR}$), the $SPA1_{STR}$-modified fiber surface was regenerated by utilizing 0.5 % SDS buffer to wash off attached $SPA2_{STR}$ and STR after each measurement. This EWF biosensing platform has been reused 100 times (each time being treated with 100 nM STR) and maintained good regeneration performance. As shown in Fig. 5c, the normalized signals of the 50th, 75th, and 100th tests were 98 %, 98 %, and 96 %, respectively, and the loss of the fluorescence signal was less than 5% after 100 tests. The regeneration results demonstrated satisfactory accuracy and reusability of this biosensor and indicated the application potential in automatic and on-line monitoring for targets, which is critical for environmental monitoring and that in other fields.

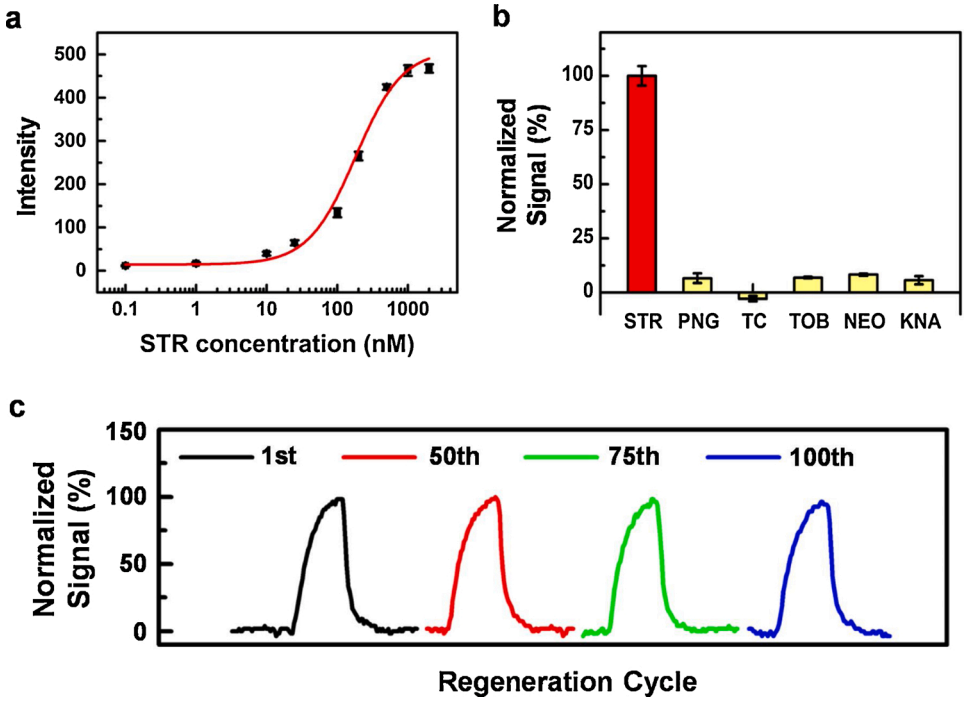

Fig. 5. Performance evaluation of the biosensor. (a) Standard detection curve of the STR detection system. (b) Normalized fluorescence intensity in the presence of 100 nM individual antibiotics. (c) Regeneration of the $SPA1_{STR}$-modified EWF biosensing interface.

3.6. Environmental samples

To investigate the practicality of the established STR detection method, the recovery study of this SPA-based biosensor was performed in five types of real-water samples, including mineral spring water, bottled purified water, tap water, surface water, and wastewater. All water samples were mixed with Tris-HCl buffer to maintain proper pH and ion concentrations for detection, and spiked with or without STR, respectively. Two spiked concentrations (50 nM, 200 nM) were chosen according to the sensitivity of our developed biosensor, and selected concentrations were within the universal concentration range (ng L^{-1}–μg L^{-1} levels) of antibiotics detected in Chinese water samples (Bu et al., 2013). The concentrations measured by this EWF biosensing platform were compared with spiked concentrations, and results are listed in Table 3. When the non-spiked samples were pumped into the EWF biosensor, no significant change in fluorescent intensity was captured, indicating that STR was not detected in any samples. For spiked samples, both for the case of low and high STR concentrations, the calculated STR concentrations were close to original spiked values. It was noted that the recovery rates in the surface water were lower than in the other samples. It noteworthy that the recovery of STR in the surface water was significantly lower than in the other samples. Considering that Hetang Lake where the surface water sample was obtained is in a vigorous state of algal growth, the colored and fluorescent substances produced by the algae could be one of the possible reasons affecting the biosensor signal. In summary, the recovery rates of STR ranged from 79.2 %–96.8 %, demonstrating the satisfactory accuracy of this biosensor and indicating the application potential in real-water samples with a simple pre-treatment.

Table 3
Recovery study of STR in spiked water samples.

Sample	Found (nM)	Spiked (nM)	Recovered (nM)	Recovery (%)
Purified water	not detected	50	43.6 ± 1.8	87.2
		200	182.8 ± 1.3	91.4
Mineral spring water	not detected	50	44.9 ± 2.6	89.8
		200	179.5 ± 2.4	89.8
Tap water	not detected	50	42.8 ± 1.9	85.6
		200	173.1 ± 2.1	86.6
Surface water	not detected	50	39.6 ± 1.2	79.2
		200	164.0 ± 1.9	82.0
Waste water	not detected	50	48.4 ± 0.4	96.8
		200	191.4 ± 11.4	95.7

4. Conclusion

To meet the needs for on-site analyses or automatic water-quality monitoring of STR, it is of great importance to develop a sensing method for STR detection with no pre-reaction, low cost, and good reusability. In this study, by combining an effective STR-specific SPA with an evanescent wave fluorescence sensing platform, we established an SPA-based sandwich-type biosensor for the detection of STR. This established biosensor has advantages of high sensitivity, simple operation, stable regeneration, and fast detection speed (< 5 min per sample). Using the sandwich-type recognition of $SPA1_{STR}$ and $SPA2_{STR}$, the LoDs of STR was as low as 33 nM, and the sensing method was sensitive in the linear range of 60–526 nM. This biosensor was highly selective to STR over that of five additional common antibiotics, and also exhibited good reusability for at least 100 uses. Considering that STR in real-water samples was determined with recovery rates from 79.2 %–96.8 %, this SPA-based fluorescent biosensor without pre-reaction could be applied in the practical measurement of STR. Moreover, because of the lack of introduction of any extra oligonucleotides or accessory materials, this SPA-based biosensing method exhibits potential promise for developing simple, sensitive, and low-cost biosensors targeting other small-molecule pollutants.

CRediT authorship contribution statement

Qian Zhu: Methodology, Investigation, Visualization, Writing - original draft. **Lanhua Liu:** Investigation. **Ruoyu Wang:** Conceptualization, Investigation. **Xiaohong Zhou:** Writing - review & editing, Supervision, Project administration, Funding acquisition, Conceptualization.

Declaration of Competing Interest

The authors report no declarations of interest.

Acknowledgement

This work is supported by Beijing Natural Science Foundation-Haidian Primitive Innovation Joint Fund Project (L182045).

Appendix A. Supplementary data

Supplementary material related to this article can be found, in the online version, at doi:https://doi.org/10.1016/j.jhazmat.2020.123941.

References

Abbasi, H., Hellenäs, K.-E., 1998. Modified determination of dihydrostreptomycin in kidney, muscle and milk by HPLC. Analyst 123, 2725–2727.
Abdul Ghaffar Memon, X.Z., Xing, Yunpeng, Wang, Ruoyu, Liu, Lanhua, Khan, Mohsin, He, Miao, 2019. Label-free colorimetric nanosensor with improved sensitivity for Pb2+ in water by using a truncated 8-17 DNAzyme. Front. Environ. Sci. Eng. 13, 12.
Asnaashari, M., Esmaeilzadeh Kenari, R., Farahmandfar, R., Taghdisi, S.M., Abnous, K., 2018. Fluorescence quenching biosensor for acrylamide detection in food products based on double-stranded DNA and gold nanoparticles. Sens. Actuators, B 265, 339–345.
Bai, Y., Feng, F., Zhao, L., Chen, Z., Wang, H., Duan, Y., 2014. A turn-on fluorescent aptasensor for adenosine detection based on split aptamers and graphene oxide. Analyst 139, 1843–1846.
Bayramoglu, G., Ozalp, V.C., Yilmaz, M., Guler, U., Salih, B., Arica, M.Y., 2015. Lysozyme specific aptamer immobilized MCM-41 silicate for single-step purification and quartz crystal microbalance (QCM)-based determination of lysozyme from chicken egg white. Microporous Mesoporous Mater. 207, 95–104.
Bayramoglu, G., Ozalp, V.C., Oztekin, M., Arica, M.Y., 2019a. Rapid and label-free detection of Brucella melitensis in milk and milk products using an aptasensor. Talanta 200, 263–271.
Bayramoglu, G., Ozalp, C., Oztekin, M., Guler, U., Salih, B., Arica, M.Y., 2019b. Design of an aptamer-based magnetic adsorbent and biosensor systems for selective and sensitive separation and detection of thrombin. Talanta 191, 59–66.
Bu, Q., Wang, B., Huang, J., Deng, S., Yu, G., 2013. Pharmaceuticals and personal care products in the aquatic environment in China: a review. J. Hazard. Mater. 262, 189–211.
Capodaglio, A.G., Callegari, A., Molognoni, D., 2016. Online monitoring of priority and dangerous pollutants in natural and urban waters: a state-of-the-art review. Manage. Environ. Qual. 27.
Chen, A., Yan, M., Yang, S., 2016. Split aptamers and their applications in sandwich aptasensors. TrAC Trends Anal. Chem. 80, 581–593.
Chen, J., Zeng, L., 2013. Enzyme-amplified electronic logic gates based on split/intact aptamers. Biosens. Bioelectron. 42, 93–99.
Cheng, S., Zheng, B., Wang, M., Lam, M.H.W., Ge, X., 2013. Double-functionalized gold nanoparticles with split aptamer for the detection of adenosine triphosphate. Talanta 115, 506–511.
Danesh, N.M., Ramezani, M., Emrani, A.S., Abnous, K., Taghdisi, S.M., 2016. A novel electrochemical aptasensor based on arch-shape structure of aptamer-complimentary strand conjugate and exonuclease I for sensitive detection of streptomycin. Biosens. Bioelectron. 75, 123–128.
Emrani, A.S., Danesh, N.M., Lavaee, P., Ramezani, M., Abnous, K., Taghdisi, S.M., 2016. Colorimetric and fluorescence quenching aptasensors for detection of streptomycin in blood serum and milk based on double-stranded DNA and gold nanoparticles. Food Chem. 190, 115–121.
Feng, C., Dai, S., Wang, L., 2014a. Optical aptasensors for quantitative detection of small biomolecules: a review. Biosens. Bioelectron. 59, 64–74.
Feng, L., Zhang, Z., Ren, J., Qu, X., 2014b. Functionalized graphene as sensitive electrochemical label in target-dependent linkage of split aptasensor for dual detection. Biosens. Bioelectron. 62, 52–58.
Ferguson, J.P., Baxter, G.A., McEvoy, J.D.G., Stead, S., Rawlings, E., Sharman, M., 2002. Detection of streptomycin and dihydrostreptomycin residues in milk, honey and meat samples using an optical biosensor. Analyst 127, 951–956.

Hong, P., Li, W., Li, J., 2012. Applications of aptasensors in clinical diagnostics. Sensors 12, 1181–1193.
Kronick, M.N., Little, W.A., 1975. A new immunoassay based on fluorescence excitation by internal reflection spectroscopy. J. Immunol. Methods 8, 235–240.
Li, Q.-m., Gao, L.-x., 2008. A novel method for the determination of streptomycin using sodium nitroprusside as a chromogenic reagent by spectrophotometry. Anal. Lett. 41, 2595–2607.
Lin, B., Yu, Y., Cao, Y., Guo, M., Zhu, D., Dai, J., Zheng, M., 2018. Point-of-care testing for streptomycin based on aptamer recognizing and digital image colorimetry by smartphone. Biosens. Bioelectron. 100, 482–489.
Liu, L.H., Zhou, X.H., Xu, W.Q., Song, B.D., Shi, H.C., 2014. Highly sensitive detection of sulfadimidine in water and dairy products by means of an evanescent wave optical biosensor. RSC Adv. 4, 60227–60233.
Liu, L.H., Zhou, X.H., Shi, H.C., 2015. Portable optical aptasensor for rapid detection of mycotoxin with a reversible ligand-grafted biosensing surface. Biosens. Bioelectron. 72, 300–305.
Liu, L., Zhou, X., Lu, M., Zhang, M., Yang, C., Ma, R., Memon, A.G., Shi, H., Qian, Y., 2017a. An array fluorescent biosensor based on planar waveguide for multi-analyte determination in water samples. Sens. Actuators, B 240, 107–113.
Liu, L., Zhou, X., Wilkinson, J.S., Hua, P., Song, B., Shi, H., 2017b. Integrated optical waveguide-based fluorescent immunosensor for fast and sensitive detection of microcystin-LR in lakes: optimization and analysis. Sci. Rep. 7.
Liu, J., Zhou, X., Shi, H., 2018. An optical biosensor-based quantification of the microcystin synthetase a gene: early warning of toxic cyanobacterial blooming. Anal. Chem. 90, 2362–2368.
Long, F., He, M., Shi, H.C., Zhu, A.N., 2008. Development of evanescent wave all-fiber immunosensor for environmental water analysis. Biosens. Bioelectron. 23, 952–958.
Mehlhorn, A., Rahimi, P., Joseph, Y., 2018. Aptamer-based biosensors for antibiotic detection: a review. Biosensors 8, 54.
Meirinho, S.G., Dias, L.G., Peres, A.M., Rodrigues, L.R., 2016. Voltammetric aptasensors for protein disease biomarkers detection: a review. Biotechnol. Adv. 34, 941–953.
Mohammad Danesh, N., Ramezani, M., Sarreshtehdar Emrani, A., Abnous, K., Taghdisi, S.M., 2016. A novel electrochemical aptasensor based on arch-shape structure of aptamer-complimentary strand conjugate and exonuclease I for sensitive detection of streptomycin. Biosens. Bioelectron. 75, 123–128.
Nguyen, P.L., Sekhon, S.S., Ahn, J.Y., Ko, J.H., Lee, L., Cho, S.J., Min, J., Kim, Y.H., 2017. Aptasensor for environmental monitoring. Toxicol. Environ. Health Sci. 9, 89–101.
Nick, T.A., De Oliveira, T.E., Pilat, D.W., Spenkuch, F., Butt, H.J., Helm, M., Netz, P.A., Berger, R., 2016. Stability of a split streptomycin binding aptamer. J. Phys. Chem. B 120, 6479–6489.
Ozalp, V.C., Bayramoglu, G., Erdem, Z., Arica, M.Y., 2015. Pathogen detection in complex samples by quartz crystal microbalance sensor coupled to aptamer functionalized core–shell type magnetic separation. Anal. Chim. Acta 853, 533–540.
Paniel, N., Baudart, J., Hayat, A., Barthelmebs, L., 2013. Aptasensor and genosensor methods for detection of microbes in real world samples. Methods 64, 229–240.
Piganeau, N., Schroeder, R., 2003. Aptamer structures: a preview into regulatory pathways? Chem. Biol. 10, 103–104.
Ping, J., Zhou, Y., Wu, Y., Papper, V., Boujday, S., Marks, R.S., Steele, T.W.J., 2015. Recent advances in aptasensors based on graphene and graphene-like nanomaterials. Biosens. Bioelectron. 64, 373–385.
Preu, M., Petz, M., 1999. Development and optimisation of a new derivatisation procedure for gas chromatographic–mass spectrometric analysis of dihydrostreptomycin: comparison of multivariate and step-by-step optimisation procedures. J. Chromatogr. A 840, 81–91.
Song, B., Shi, H., He, M., Zhang, F., Guo, B., 2007. Optical immuno-sensors chip for environmental monitoring and food security detection. Qinghua Daxue Xuebao 47, 847–850.
Strehlitz, B., Reinemann, C., Linkorn, S., Stoltenburg, R., 2012. Aptamers for pharmaceuticals and their application in environmental analytics. Bioanal. Rev. 4, 1–30.
Taghdisi, S.M., Danesh, N.M., Nameghi, M.A., Ramezani, M., Abnous, K., 2016. A label-free fluorescent aptasensor for selective and sensitive detection of streptomycin in milk and blood serum. Food Chem. 203, 145–149.
Taitt, C.R., Anderson, G.P., Ligler, F.S., 2005. Evanescent wave fluorescence biosensors. Biosens. Bioelectron. 20, 2470–2487.
Tereshko, V., Skripkin, E., Patel, D.J., 2003. Encapsulating streptomycin within a small 40-mer RNA. Chem. Biol. 10, 175–187.
van Bruijnsvoort, M., Ottink, S.J., Jonker, K.M., de Boer, E., 2004. Determination of streptomycin and dihydrostreptomycin in milk and honey by liquid chromatography with tandem mass spectrometry. J. Chromatogr. A 1058, 137–142.
Wallace, S.T., Schroeder, R., 1998. In vitro selection and characterization of streptomycin-binding RNAs: recognition discrimination between antibiotics. RNA (New York, N.Y.) 4, 112–123.
Wang, R., Xiang, Y., Zhou, X., Liu, L.H., Shi, H., 2015a. A reusable aptamer-based evanescent wave all-fiber biosensor for highly sensitive detection of Ochratoxin A. Biosens. Bioelectron. 66, 11–18.
Wang, R., Zhou, X., Shi, H., 2015b. Triple functional DNA-protein conjugates: signal probes for Pb2+ using evanescent wave-induced emission. Biosens. Bioelectron. 74, 78–84.
Wang, R., Zhou, X., Shi, H., 2015c. Triple functional DNA–protein conjugates: signal probes for Pb2+ using evanescent wave-induced emission. Biosens. Bioelectron. 74, 78–84.
Wang, R., Zhou, X., Shi, H., Luo, Y., 2016a. T-T mismatch-driven biosensor using triple functional DNA-protein conjugates for facile detection of Hg2+. Biosens. Bioelectron. 78, 418–422.
Wang, R., Zhou, X., Shi, H., Luo, Y., 2016b. T–T mismatch-driven biosensor using triple functional DNA-protein conjugates for facile detection of Hg2+. Biosens. Bioelectron. 78, 418–422.
Wang, R., Zhou, X., Zhu, X., Yang, C., Liu, L., Shi, H., 2017. Isoelectric bovine serum albumin: robust blocking agent for enhanced performance in optical-fiber based DNA sensing. ACS Sens. 2, 257–262.
Wang, Z., Yu, H., Canoura, J., Liu, Y., Alkhamis, O., Fu, F., Xiao, Y., 2018. Introducing structure-switching functionality into small-molecule-binding aptamers via nuclease-directed truncation. Nucleic Acids Res. 46 e81-e81.
Wang, R., Zhang, Q., Zhang, Y., Shi, H., Nguyen, K.T., Zhou, X., 2019. Unconventional split aptamers cleaved at functionally essential sites preserve biorecognition capability. Anal. Chem. 91, 15811–15817.
Wu, C., Yang, S., Wu, Z., Shen, G., Yu, R., 2013. Split aptamer-based liquid crystal biosensor for ATP assay. Acta Chim. Sin. 71, 367–370.
Xu, X., Liu, D., Luo, L., Li, L., Wang, K., You, T., 2017. Photoelectrochemical aptasensor based on CdTe quantum dots-single walled carbon nanohorns for the sensitive detection of streptomycin. Sens. Actuators B Chem. 251, 564–571.
Yagur-Kroll, S., Schreuder, E., Ingham, C.J., Heideman, R., Rosen, R., Belkin, S., 2015. A miniature porous aluminum oxide-based flow-cell for online water quality monitoring using bacterial sensor cells. Biosens. Bioelectron. 64, 625–632.
Yamamoto-Fujita, R., Kumar, P.K., 2005. Aptamer-derived nucleic acid oligos: applications to develop nucleic acid chips to analyze proteins and small ligands. Anal. Chem. 77, 5460–5466.
Yang, C., Spinelli, N., Perrier, S., Defrancq, E., Peyrin, E., 2015. Macrocyclic host-dye reporter for sensitive sandwich-type fluorescent aptamer sensor. Anal. Chem. 87, 3139–3143.
Yin, J., Guo, W., Qin, X., Pei, M., Feng, D., 2016. A regular "signal attenuation" electrochemical aptasensor for highly sensitive detection of streptomycin. New J. Chem. 40, 9711–9718.
Zhang, J., Wang, L., Pan, D., Song, S., Boey, F.Y.C., Zhang, H., Fan, C., 2008. Visual cocaine detection with gold nanoparticles and rationally engineered aptamer structures. Small 4, 1196–1200.
Zhou, N., Wang, J., Zhang, J., Li, C., Tian, Y., Wang, J., 2013. Selection and identification of streptomycin-specific single-stranded DNA aptamers and the application in the detection of streptomycin in honey. Talanta 108, 109–116.
Zuo, X., Xiao, Y., Plaxco, K.W., 2009. High specificity, electrochemical sandwich assays based on single aptamer sequences and suitable for the direct detection of small-molecule targets in □ blood and other complex matrices. J. Am. Chem. Soc. 131, 6944–6945.